Available online at www.sciencedirect.com
ScienceDirect
Microelectronic Engineering 85 (2008) 247–252
MICROELECTRONIC ENGINEERING
www.elsevier.com/locate/mee

Frequency and voltage effects on the dielectric properties and electrical conductivity of Al–TiW–Pd_2Si/n-Si structures

İ.M. Afandiyeva [a], İ. Dökme [b,*], Ş. Altındal [c], M.M. Bülbül [c], A. Tataroğlu [c]

[a] Bakü State University, Institute of Physics Problems, AZ 1148 Baku, Azerbaijan
[b] Science Education Department, Faculty of Education, Ahi Evran University, Kırşehir, Turkey
[c] Physics Department, Faculty of Arts and Sciences, Gazi University, 06500 Teknikokullar, Ankara, Turkey

Received 25 February 2007; received in revised form 7 May 2007; accepted 25 May 2007
Available online 2 June 2007

Abstract

Different from conventional metal–Si compounds–n-Si structures, the thin film of TiW alloy was deposited on Pd_2Si–n-Si to form a diffusion barrier between aluminum (Al) and Pd_2Si–n-Si. Dielectric properties and electrical conductivity of TiW–Pd_2Si/n-Si structures in the frequency range of 5 kHz–10 MHz and voltage range of (−4 V) to (10 V) have been investigated in detail by using experimental *C–V* and *G–V* measurements. Experimental results indicate that the values of ε' show a steep decrease with increasing frequency for each voltage. On the other hand, the values of ε'' show a peak, and its intensity increases with decreasing voltage and shifts towards the lower frequency side. The ac electrical conductivity (σ_{ac}) and the real part of electric modulus (M') increase with increasing frequency. Also, the imaginary part of electric modulus (M'') shows a peak and the peak position shifts to higher frequency with increasing applied voltage. It can be concluded that the interfacial polarization can be more easily occurred at low frequencies, and the majority of interface states at metal semiconductor interface, consequently contributes to deviation of dielectric properties of TiW–Pd_2Si/n-Si structures.
© 2007 Elsevier B.V. All rights reserved.

Keywords: Al–TiW–Pd_2Si/n-Si; $Ti_{10}W_{90}$ thin film; Dielectric properties; Electric modulus; ac electrical conductivity

1. Introduction

The interface structure between metal and semiconductor plays a very important role in the fabrication of metal–semiconductor (MS) and metal–insulator–semiconductor (MIS) structures. These devices have been gaining importance due to their wide variety opto-electronic and high-frequency applications [1,2]. The performance and reliability of these devices especially depend on the formation of interface structure between metal and semiconductor. During fabrication process of MS structures, an oxide layer can be formed on Si by natural ways [3–7]. However, an insulator interfacial layer or silicide compounds at metal–Si interfaces can be formed on Si by different technique to passivate interfacial-contamination arisen from the active dangling bonds at the semiconductor surface [8]. Most of the properties of the non-reacting interface, e.g. Al–Si, may be characteristics of the discrete nature of the ideal metal–Si interface. In addition to this, the silicide compound formation process at a reaction interface which is created continuously by atomic rearrangement resulting from material reaction. This tends to better preserve the intrinsic characteristics of the interface since it is less susceptible to interfacial-contamination effects [9]. In this respect, the interfacial parameters such as the density of interface states and the thickness of interfacial layer can influence both the electrical and dielectric behavior of these structures [10–20]. In the ideal case, the capacitance of MS or MIS structures is usually frequency independent especially at high frequency limit ($f \geqslant 1$ MHz). Depending on the frequency of the a.c signal, there may be a capacitance due to interface states in excess to depletion layer

* Corresponding author. Tel.: +90 3122155471; fax: +90 3862134513.
E-mail address: ilbilgedokme@gazi.edu.tr (İ. Dökme).

0167-9317/$ - see front matter © 2007 Elsevier B.V. All rights reserved.
doi:10.1016/j.mee.2007.05.044

capacitance. When localized interface states exist at the interface, the device behavior is different than ideal case due to their presence. Since the interface capacitance (excess capacitance) depend on strongly on the frequency and applied voltage, the C–V and G/w–V characteristics are strongly affected [1,10–24]. Therefore, it is important to include the effect of voltage and frequency in the investigation of both electrical and dielectric properties [20–26]. The frequency response of the dielectric constant (ε'), dielectric loss (ε'') and loss tangent ($\tan\delta$) is dominated by a low frequency dispersion, whose physical origin has long been in question [27].

In this work, Al–TiW–Pd_2Si/n-Si structures were first fabricated and then both the forward and reverse bias admittance measurements were studied over the frequency and voltage range of 5 kHz–10 MHz and −4V to 10 V, respectively, by using an HP-4192 A impedance analyzer at room temperature. The variation of dielectric constant (ε'), dielectric loss (ε''), loss tangent ($\tan\delta$), ac electrical conductivity (σ_{ac}) and real and imaginary part of electric modulus (M' and M) have been investigated as a function of frequency and voltage.

2. Experimental procedure

The Al–TiW–Pd_2Si/n-Si structures were fabricated on 2 in. diameter n-type (P doped) single crystal silicon wafer with (1 1 1) surface orientation, 0.7 Ω cm resistivity and 3.5 μm thickness. The pattern of these structures were fabricated by lift-off of litho-graphically system, defined as photo-resist, and annealed at 500 C for 1 min in flowing dry nitrogen (N_2) ambient in a rapid thermal annealing furnace. Thus produced chip contains 14 Al–TiW–Pd_2Si/n-Si structures with the areas of changing 1×10^{-6} cm^2–14×10^{-6} cm^2. Only the results of diode with the area of 8×10^{-6} cm^2 are presented in this paper.

For the fabrication process the Si wafer first was cleaned in a mix of a peroxide–ammoniac solution in 10 min and subsequent quenched in de-ionized water of resistivity of 18 MΩ cm for a prolonged time. After the cleaning process, high purity (99.999%) Al with a thickness of about 2000 Å were thermally evaporated onto whole back side of Si wafer at a pressure about 10^{-6} Torr in high vacuum system. The ohmic contacts were formed by annealing them for a few minutes at 450 °C. To fabricate Pd_2Si–n-Si layer, palladium was deposited on Si wafer by using thermal evaporation method until the thickness of Pd_2Si film was about 0.6 μm, subsequently annealed at 573 K for 15 min. To form the metal electrodes (rectifier and ohmic contacts), traditionally Al dot could have been formed on Pd_2Si–n-Si structure. But Al has high diffusion ability and it can lead to degrade contact's quality. Therefore in this work, to prevent the disadvantage of Al diffusion to n-Si, the TiW alloy played the role of the diffusion barrier between Pd_2Si, and Al was deposited on Pd_2Si–n-Si layer. For this process, the sandwiched structure Al–$Ti_{10}W_{90}$ was deposited by the magnetron sputtering method at temperature of 420 °C in vacuum system 'Oratoria-5' and then annealed at temperature of 500 °C in nitrogen atmosphere (N_2) for 20 min. Prior to the deposition, vacuum and target conditions were performed. Taking into account the dispersion factor of Ti and W, the compound target (Ti 10%, W 90%) were made. The deposition chamber was pumped down to the ultimate vacuum and repeatedly charged with argon and pumped down in order to minimize the residual gas components. The alloy compound target film was bombarded by Ar^+ ions with high energy at room temperature until the thickness of $Ti_{10}W_{90}$ film on Pd_2Si–n-Si substrate was about 0.2 μm. The base pressure during the ion bombardments was about 10^{-6} Torr. Al was also deposited onto TiW–Pd_2Si/n-Si structure by the same method until the thickness of Al film on $Ti_{10}W_{90}$-Pd2Si–n-Si layer was about 1 μm.

The C–V ang G/ω–V measurements were performed in the frequency range of 5 kHz–10 MHz by using a HP 4192A LF impedance analyzer and small sinusoidal test signal of 20 mV$_{p-p.}$ from the external pulse generator is applied to the sample in order to meet the requirement. All measurements were carried out with the help of a microcomputer through an IEEE-488 ac/dc converter card.

3. Results and discussion

The frequency dependence of dielectric constant (ε'), dielectric loss (ε''), loss tangent ($\tan\delta$), ac electrical conductivity (σ_{ac}) and electric modulus were evaluated from the knowledge of capacitance and conductance measurements for Al–TiW–Pd_2Si/n-Si structures in the frequency range of 5 kHz–10 MHz, at room temperature. The complex permittivity can be written [22,23] as

$$\varepsilon^* = \varepsilon' - i\varepsilon'' \tag{1}$$

where ε' and ε'' are the real and imaginary of complex permittivity, and i is the imaginary root of −1. The complex permittivity formalism has been employed to describe the electrical and dielectric properties. In the ε^* formalism, in the case of admittance Y^* measurements, the following relation holds

$$\varepsilon^* = \frac{Y^*}{j\omega C_o} = \frac{C}{C_o} - i\frac{G}{\omega C_{oi}} \tag{2}$$

where C and G are the measured capacitance and conductance of the device, ω is the angular frequency ($\omega = 2\pi f$) of the applied electric field [28]. The real part of the complex permittivity, the dielectric constant (ε'), at the various frequencies is calculated using the measured capacitance values at the strong accumulation region from the relation [17,25],

$$\varepsilon' = \frac{C}{C_o} = \frac{Cd_i}{\varepsilon_o A} \tag{3}$$

where C_o is capacitance of an empty capacitor, A is the rectifier contact area of the structure in cm^{-2}, d_i is the interfacial insulator layer thickness and ε_o is the permittivity of free space charge ($\varepsilon_o = 8.85\times10^{-14}$ F/cm). In the strong

accumulation region, the maximal capacitance of the structure corresponds to the insulator capacitance ($C_{ac} = C_i = \varepsilon' \ \varepsilon_o A/d_i$). The imaginary part of the complex permittivity, the dielectric loss (ε''), at the various frequencies is calculated using the measured conductance values from the relation,

$$\varepsilon'' = \frac{G}{\omega C_i} = \frac{G d_i}{\varepsilon_o \omega A} \quad (4)$$

The loss tangent ($\tan\delta$) can be expressed as follows [17,22–25],

$$\tan\delta = \frac{\varepsilon''}{\varepsilon'} \quad (5)$$

The ac electrical conductivity (σ_{ac}) of the dielectric material can be given by the following equation: [22,28,29],

$$\sigma_{ac} = \omega C \tan\delta(d/A) = \varepsilon''\omega\varepsilon_o \quad (6)$$

The complex impedance (Z^*) and complex electric modulus (M^*) formalisms were discussed by various authors with regard to the analysis of dielectric materials [18,22]. Analysis of the complex permittivity (ε^*) data in the Z^* formalism ($Z^* = 1/Y^* = 1/\mathrm{i}\omega C_o\varepsilon^*$) is commonly used to separate the bulk and the surface phenomena and to determine the bulk dc conductivity of the material [24,28]. Many authors prefer to describe the dielectric properties of these devices by using the electric modulus formalize [29,30]. The complex impedance or the complex permittivity ($\varepsilon^* = 1/M^*$) data are transformed into the M^* formalism using the following relation [29–32]

$$M^* = \mathrm{i}\omega C_o Z^* \quad (7)$$

or

$$M^* = \frac{1}{\varepsilon^*} = M' + jM'' = \frac{\varepsilon'}{\varepsilon'^2 + \varepsilon''^2} + j\frac{\varepsilon''}{\varepsilon'^2 + \varepsilon''^2} \quad (8)$$

The real component M' and the imaginary component M' are calculated from ε' and ε''. Fig. 1 shows the voltage dependence of the real part of dielectric constant (ε) of the Al–TiW–Pd_2Si/n-Si structure at various frequencies. It is noticed that the values of ε' increase with decreasing frequency and tend to be frequency independent at low voltages. The decrease in ε' with increasing frequency may be attributed to the polarization decreasing with increasing frequency and then reaches a constant value due to the fact that beyond a certain frequency of external field the electron hopping cannot follow the alternative field. The dispersion in ε' with frequency can be attributed to Maxwell–Wagner type interfacial polarization, i.e. the fact that inhomogeneities give rise to a frequency dependence of the conductivity because charge carries accumulate at the boundaries of less conducting regions, thereby creating interfacial polarization [17]. Figs. 2 and 3 show the voltage dependence of dielectric loss (ε'') and the loss tangent ($\tan\delta$) of the TiW–Pd_2Si/n-Si structure at various

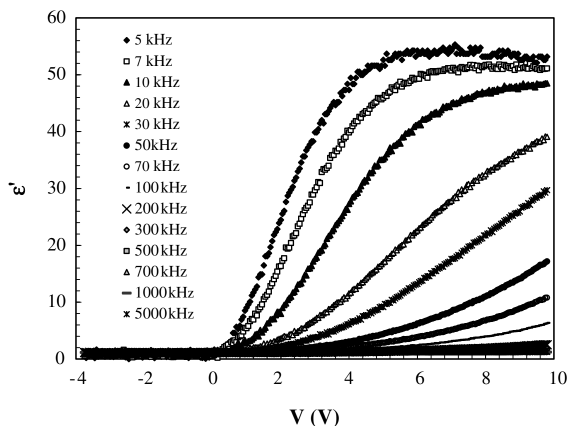

Fig. 1. The variations of the dielectric constant vs applied voltage for various frequencies of Al–TiW–Pd_2Si/n-Si structure at room temperature.

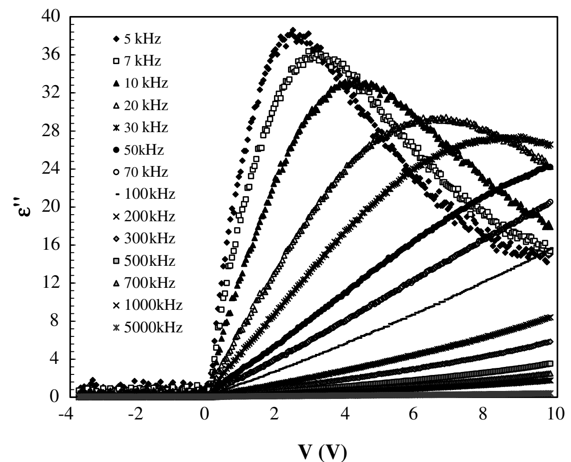

Fig. 2. The variations of dielectric loss vs applied voltage for various frequencies of Al–TiW–Pd_2Si/n-Si structure at room temperature.

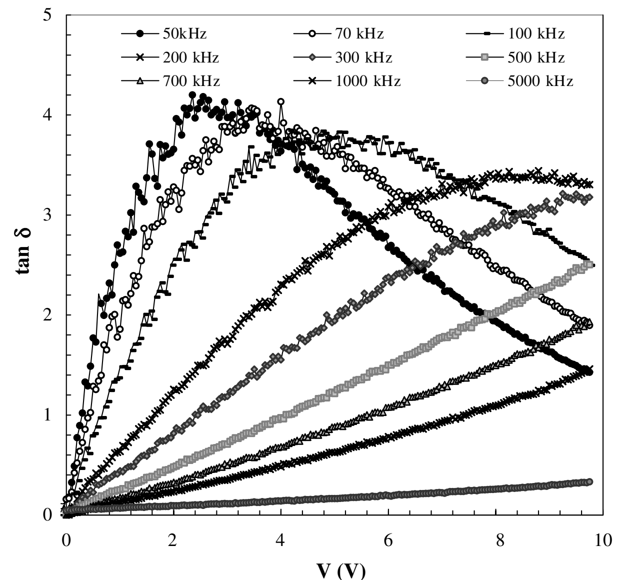

Fig. 3. The variations of tangent loss vs applied voltage for various frequencies of Al–TiW–Pd_2Si/n-Si structure at room temperature.

frequencies. As can be seen in these figures, the values of ε'' and $\tan\delta$ are strongly dependent on both frequency and applied bias voltage. The ε''–V and $\tan\delta$–V characteristics have a peak especially at low frequency. The peak values of ε''–V and $\tan\delta$–V have decreased with increasing frequency and the peak positions strongly shift towards negative bias region.

The peak behavior of the ε'' and $\tan\delta$ depend on a number of parameters such as doping concentration, interface state density, series resistance of diode and the thickness of the interfacial insulator layer [33]. It is well known that the capacitance and conductance are extremely sensitive to the interface properties and series resistance [10,21]. This occurs because of the interface states that respond differently to low and high frequencies. Similar results have been reported in the literature [8,19,21,24] and they ascribed such a peak to only interface states.

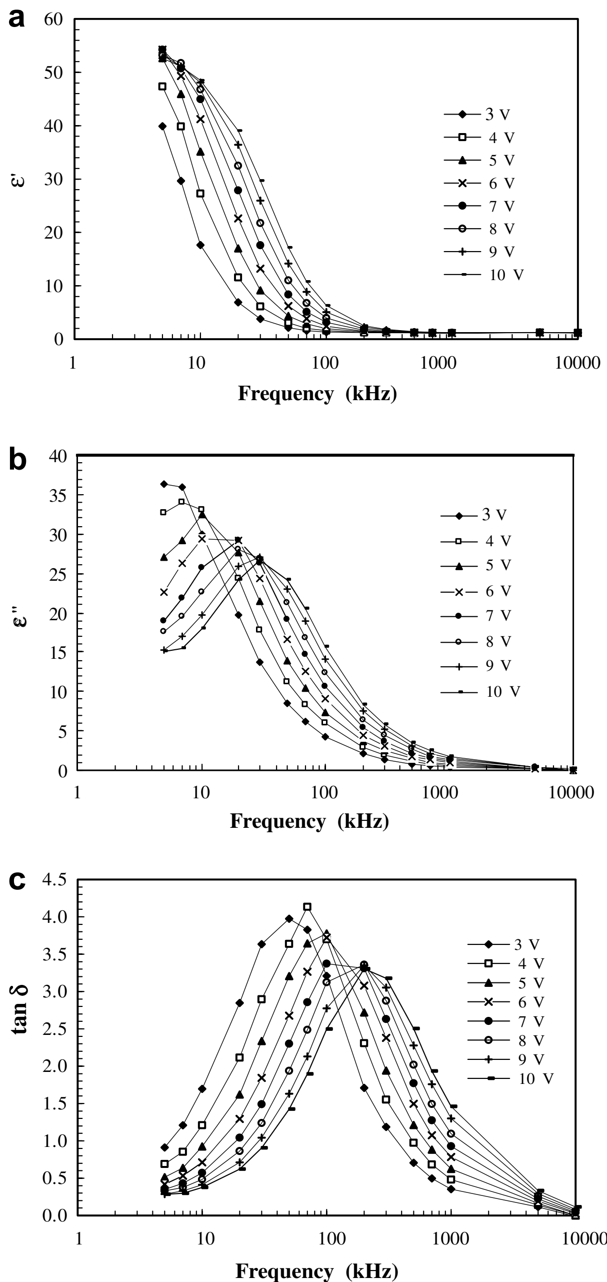

Fig. 4. Frequency dependence of the (a) ε', (b) ε'' and (c) $\tan\delta$ for various applied voltage of Al–TiW–Pd_2Si/n-Si structure at room temperature.

The frequency dependence of the ε', ε'' and $\tan\delta$ of Al–TiW–Pd_2Si/n-Si at different voltage are presented in Fig. 4a, b and c, respectively. The values of the ε', ε'' and $\tan\delta$ obtained from the measured capacitance and conductance were found a strong function of applied voltage especially at low frequencies. As shown in Fig. 4a, the values of ε' show a steep decrease with increasing frequency for each voltage. On the other hand, the values of ε'' (Fig. 4b) show a broad peak, and its intensity increases with decreasing voltage and shifts towards the lower frequency side.

The peak values of $\tan\delta$–f (Fig. 4c) have decreased with increasing voltage and the peak positions tend to shift towards high frequency region. Also, it is clearly seen in Fig. 4, that the values of ε', ε'' and $\tan\delta$ of Al–TiW–Pd_2Si/n-Si are almost independent of voltage at high frequencies. In principle, at low frequencies, all the four types of polarization processes, i.e. the electronic, ionic, dipolar, and interfacial or surface polarization contribute to the values of ε' and ε''. In addition, at high frequencies the values of ε' become closer to the values of ε'' due to the interface states (N_{ss}) cannot follow the ac signal at enough high frequency ($f \geqslant 500$ kHz) [33–36].

The behavior of ac electrical conductivity (σ_{ac}) of the Al–TiW–Pd_2Si/n-Si structure at different voltage is presented in Fig. 5. It is noticed that the electrical conductivity generally increases with increasing frequency at low frequencies up to 30 kHz, and after this frequency it is independent of frequency for each voltage. This electrical conductivity contributes only to the dielectric loss, which

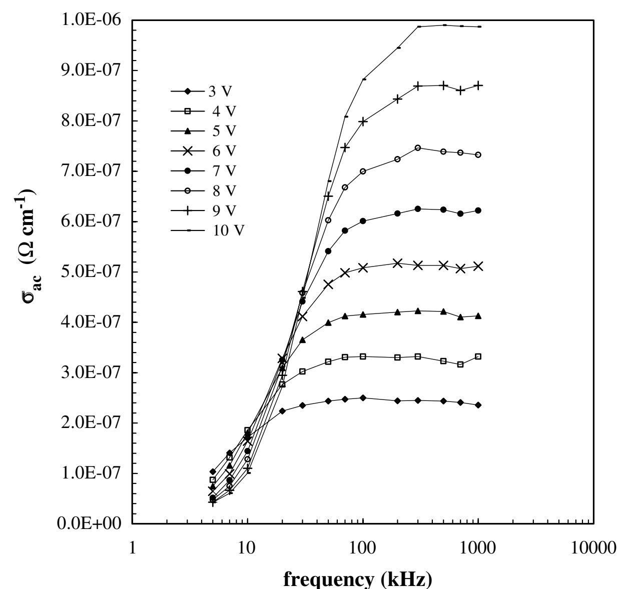

Fig. 5. Frequency dependence of ac electrical conductivity (σ_{ac}) for various applied voltage of Al–TiW–Pd_2Si/n-Si structure at room temperature.

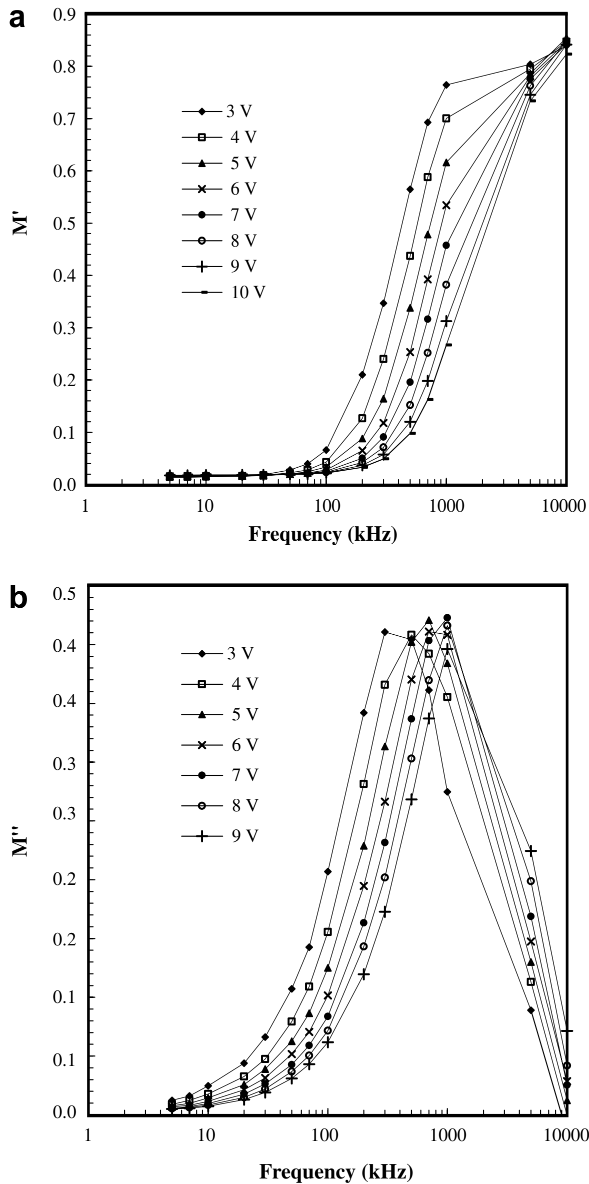

Fig. 6. (a) The real part M' and (b) the imaginary part M'' of electric modulus M^* vs frequency for Al–TiW–Pd_2Si/n-Si structure at room temperature.

becomes infinite at zero frequency and not important at high frequencies [37–40]. The increase of the electrical conductivity lead to an increase of the eddy current which in turn increases the energy loss tang δ. This behavior can be attributed to a gradual decrease in series resistance with increasing frequency [40].

The variation of the real part of electric modulus, M', and their imaginary part of M'', of Al–TiW–Pd_2Si/n-Si structure as a function of frequency at various bias voltages are given in Fig. 6a and b, respectively, at room temperature. It is evident from Fig. 6 that for each bias voltage, M' reaches a constant value at higher frequency. In other words, M' reaches a maximum constant value corresponding to $M_\infty = 1/\varepsilon_\infty$ due to the relaxation process. At low frequencies, the values of M' approach zero, confirming the removal of electrode polarization. As being different from literature [29–33], the M'' of electric modulus M^* vs f have a peak for each voltage (Fig. 6b). While there is an increase in M'' between 5 kHz and 300 kHz, there is a decrease between 300 kHz and 10 MHz. The variation of M'' with frequency at various bias voltages in Fig. 6b reveals that as frequency increases M'' increases and takes a peak value at each bias voltage between ≈200 kHz and 1 MHz. The position of peak shifts to higher frequency with increasing gate voltage.

4. Conclusions

A thin film of TiW alloy was deposited on Pd_2Si–n-Si to form the diffusion barrier in a novel Al–TiW–Pd_2Si/n-Si structure. An analysis of experimental results have shown that the values of ε' show a steep decrease with increasing frequency for each voltage while the values of ε'' show a peak, and its intensity increases with decreasing voltage and shifts towards the lower frequency side. The ac electrical conductivity (σ_{ac}) and the real part of electric modulus (M') increase with increasing frequency. Also, the imaginary part of electric modulus (M'') shows a peak and the peak position shifts to higher frequency with increasing applied voltage. It is conclude that the values of ε', ε'', $\tan\delta$, M' and M'' in Al–TiW–Pd_2Si/n-Si structure are strongly depend on both the frequency and applied bias voltage.

References

[1] S.M. Sze, Physics of Semiconductor Devices, second ed., Willey, New York, 1981.
[2] K. Kano, Semiconductor Devices, Prentice-Hall, New Jersey, 1998.
[3] P. Cova, A. Singh, A. Medina, R.A. Masut, Solid State Electron. 42 (1998) 477.
[4] H.H. Tseng, C.Y. Wu, Solid State Electron. 30 (1987) 383.
[5] M.E. Aydın, K. Akkılıc, T. Kılıçoğlu, Physica B 352 (2004) 312.
[6] P.L. Hanselaer, W.H. Laflere, R.L. Van Meirhaeghe, F. Cardon, J. Appl. Phys. 56 (1984) 2309.
[7] İ. Dökme, Physica B: Condens. Mat. 388 (2007) 10.
[8] M.M. Bülbül, Microelectron. Eng. 84 (2007) 124.
[9] P.S. Ho, G.W. Rubloff, J.E. Lewis, V.L. Moruzzi, A.R. Williams, Phys. Rev. B 22 (1980) 4784.
[10] E.H. Nicollian, J.R. Brews, MOS Physics and Technology, John Wiley and Sons, New York, 1982.
[11] H. Deuling, E. Klausmann, A. Goetzberger, Solid State Electron. 15 (5) (1972) 559.
[12] M. Depas, R.L. Van Meirhaeghe, W.H. Lafere, F. Cardon, Solid State Electron. 37 (3) (1994) 433.
[13] S. Kar, R.L. Narasimhan, J. Appl. Phys. 61 (12) (1987) 5353.
[14] S. Varma, K.V. Rao, S. Kar, J. Appl. Phys. 56 (1984) 2812.
[15] M. Schulz, E. Klausmann, Appl. Phys. 18 (1979) 169.
[16] N. Konofaos, I.P. McClean, C.B. Thomas, Phys. Stat. Sol. (a) 161 (1997) 111.
[17] A. Chelkowski, Dielectric Physics, Elsevier, Amsterdam, 1980.
[18] K.S. K Kwa, S. Chattopadhyay, N.D. Jankovic, S.H. Olsen, L.S. Driscoll, A.G. O'Niell, Semicond. Sci. Technol. 18 (2003) 82.
[19] İ. Dökme, Ş. Altındal, Physica B: Condens. Mat. 391 (2007) 59.
[20] S. Kar, W.E. Dahlke, Solid State Electron. 15 (1972) 221.
[21] E.H. Nicollian, A. Goetzberger, Appl. Phys. Lett. 7 (1965) 216.
[22] C.P. Symth, Dielectric Behaviour and Structure, McGraw-Hill, New York, 1955.

[23] Vera V. Daniel, Dielectric Relaxation, Academic Press, London, 1967.
[24] İ. Yücedağ, Ş. Altındal, A. Tataroğlu, Microelectron. Eng. 84 (2006) 180.
[25] M. Popescu, I. Bunget, Physics of Solid Dielectrics, Elsevier, Amsterdam, 1984.
[26] B. Akkal, Z. Benamara, B. Gruzza, L. Bideux, N. Bachir Bouiadjra, Mater. Sci. Eng. C 21 (2002) 291.
[27] S. Kar, S. Varma, J. Appl. Phys. 58 (11) (1985) 4256.
[28] M.S. Mattsson, G. A Niklasson, K. Forsgren, A. Harsta, J. Appl. Phys. 85 (4) (1999) 2185.
[29] K. Prabakar, S.K. Narayandass, D. Mangalaraj, Phys. Stat. Sol. (a) 199 (3) (2003) 507.
[30] P. Pissis, A. Kyritsis, Solid State Ion. 97 (1997) 105.
[31] M.D. Migahed, M. Ishra, T. Fahmy, A. Barakat, J. Phys. Chem. Solids 65 (2004) 1121.
[32] P. Chattopadhyay, B. Raychaudhuri, Solid State Electron. 35 (1992) 875.
[33] S.P. Szu, C.Y. Lin, Mater. Chem. Phys. 82 (2003) 295.
[34] D. Maurya, J. Kumar, Shripal, J. Phys. Chem. Solids 66 (2005) 1614.
[35] C.V. Kannan, S. Ganesamoorthy, C. Subramanian, P. Ramasamy, Phys. Stat. Sol. (a) 196 (2) (2003) 465.
[36] N. Konofaos, E.K. Evangelou, X. Aslanoglou, M. Kokkoris, R. Vlastou, Semicond. Sci. Technol. 19 (2004) 50.
[37] M. Cutroni, A. Mandanici, A. Piccolo, C. Fanggao, G.A. Saunders, P. Mustarelli, Solid State Electron. 90 (1996) 167.
[38] D. Maurya, J. Kumar, Shripal, J. Phys. Chem. Solids 66 (2005) 1614.
[39] A.S. Riad, M.T. Korayem, T.G. Abdel-Malik, Physica B 270 (1999) 140.
[40] A. Tataroğlu, Ş. Altındal, M.M. Bülbül, Microelectron. Eng. 81 (2005) 140.